Article

Hydrolytic Cleavage of an RNA-Model Phosphodiester Catalyzed by a Highly Negatively Charged Polyoxomolybdate [MoO]$^{-}$ Cluster

Gregory Absillis, Els Cartuyvels, Rik Van Deun, and Tatjana N. Parac-Vogt

J. Am. Chem. Soc., **2008**, 130 (51), 17400-17408 • DOI: 10.1021/ja804823g • Publication Date (Web): 02 December 2008

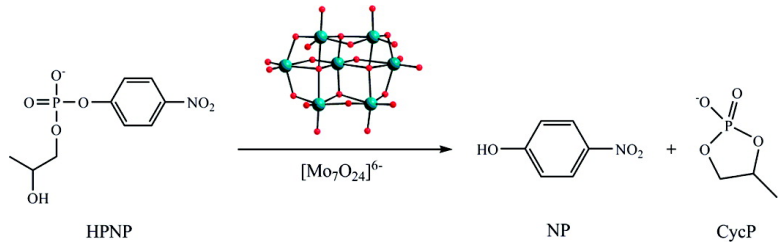

More About This Article

Additional resources and features associated with this article are available within the HTML version:

- Supporting Information
- Access to high resolution figures
- Links to articles and content related to this article
- Copyright permission to reproduce figures and/or text from this article

View the Full Text HTML

J|A|C|S
ARTICLES

Published on Web 12/02/2008

Hydrolytic Cleavage of an RNA-Model Phosphodiester Catalyzed by a Highly Negatively Charged Polyoxomolybdate $[Mo_7O_{24}]^{6-}$ Cluster

Gregory Absillis, Els Cartuyvels, Rik Van Deun,† and Tatjana N. Parac-Vogt*

Department of Chemistry, Katholieke Universiteit Leuven, Celestijnenlaan 200F, B-3001 Leuven, Belgium

Received June 24, 2008; E-mail: Tatjana.Vogt@chem.kuleuven.be

Abstract: Hydrolysis of 2-hydroxypropyl-4-nitrophenyl phosphate (HPNP), a commonly used RNA model substrate, was examined in molybdate solutions by means of ^{1}H, ^{31}P, and ^{95}Mo NMR, Raman, and Mo K-edge extended X-ray absorption fine structure (EXAFS) spectroscopy. ^{1}H and ^{31}P NMR spectroscopy indicate that at 50 °C and pD 5.9 the cleavage of the phosphodiester bond in HPNP proceeds with a rate constant of 6.62×10^{-6} s^{-1}, giving a cyclic phosphate ester and *p*-nitrophenol as the only products of hydrolysis. The NMR spectra did not show evidence of any paramagnetic species, excluding the possibility of Mo(VI) reduction to Mo(V), and indicating that the cleavage of the phosphodiester bond is purely hydrolytic. The Mo K-edge XANES region also did not show any sign of Mo(VI) to Mo(V) reduction during the hydrolytic reaction. The pD dependence of k_{obs} exhibits a bell-shaped profile, with the fastest cleavage observed at pD 5.9. Comparison of the rate profile with the concentration profile of polyoxomolybdates shows a striking overlap of the k_{obs} profile with the concentration of heptamolybdate, suggesting that the highly negatively charged $[Mo_7O_{24}]^{6-}$ is the hydrolytically active species. Kinetic experiments at pD 5.9 using a fixed amount of $[Mo_7O_{24}]^{6-}$ and increasing amounts of HPNP revealed slight signs of curvature at 25 molar excess of HPNP. The data fit the general Michaelis−Menten reaction scheme, permitting the calculation of the catalytic rate constant k_2 (3.02×10^{-4} s^{-1}) and K_m (1.06 M). Variable temperature ^{31}P NMR spectra of a reaction mixture revealed broadening of the HPNP ^{31}P resonance upon increase of temperature, implying the dynamic exchange process between free and bound HPNP at higher temperatures. Addition of salts resulted in the inhibition of HPNP hydrolysis, as well as addition of dimethyl phosphate, suggesting competition for the binding to $[Mo_7O_{24}]^{6-}$. The hydrolysis of 10 equiv of HPNP could be achieved in the presence of 1 equiv of $[Mo_7O_{24}]^{6-}$, and the multiple turnovers demonstrate that the reaction is catalytic. ^{31}P NMR and Mo K-edge EXAFS spectra measured during different stages of the hydrolysis indicated that under catalytic conditions a partial conversion of $[Mo_7O_{24}]^{6-}$ into $[P_2Mo_5O_{23}]^{6-}$ occurs.

Introduction

Polyoxometalates (POMs) represent a large class of inorganic oxo-clusters that contain early transition metals (Mo, W, V, Nb, and Ta) in their highest oxidation state. Because of their versatile chemical, structural, and electronic properties they have attracted considerable interest in the fields of homogeneous and heterogeneous catalysis, electronics, and magnetic materials.[1−4] In the past decade numerous studies have demonstrated that POMs also exhibit potent antiviral, antibacterial, and antitumor activities, initiating a substantial interest in the potential medicinal application of POMs.[5−10] Various POMs have been reported to interact with viral surface proteins and to inhibit the replication of several types of viruses including human immunodeficiency virus (HIV).[11−13] Recent studies have shown that POMs have superior ability to precipitate prion proteins, a property which could be very useful in the development of immonoassays capable of detecting extremely low concentra-

† Current address: Inorganic and Physical Chemistry Group, Ghent University.

(1) Pope, M. T.; Müller, A. *Angew. Chem., Int. Ed.* **1991**, *30*, 34.
(2) Pope, M. T. Polyoxo anions: Synthesis and Structure. In *Comprehensive Coordination Chemistry II;* Wedd, A. G., Ed.; Elsevier Science: New York, 2004; Vol. 4, pp 635−678.
(3) Hill, C. L. Polyoxometalates: Reactivity. In *Comprehensive Coordination Chemistry II*; Wedd, A. G., Ed.; Elsevier Science: New York, 2004; Vol. *4,* pp 679−759.
(4) Pope, M. T., Müller, A., Eds. *Polyoxometalate Chemistry: From Topology via Self-Assembly to Applications*; Kluwer: Dordrecht, The Netherlands, 2001.
(5) Rhule, J. T.; Hill, C. L.; Judd, D. A. *Chem. Rev.* **1998**, *98*, 327.
(6) Yamase, T. *J. Mater. Chem.* **2005**, *15*, 4773.
(7) Hasenknopf, B. *Front. Biosci.* **2005**, *10*, 275.
(8) Wang, X. H.; Li, F.; Liu, S. X.; Pope, M. T. *J. Inorg. Biochem.* **2005**, *99*, 452.
(9) Gerth, H. U. V.; Rompel, A.; Krebs, B.; Boos, J.; Lanvers-Kaminsky, C. *Anti-Cancer Drugs* **2005**, *16*, 101.
(10) Cindric, M.; Novak, T. K.; Kraljevic, S.; Kralj, M.; Kamenar, B. *Inorg. Chim. Acta* **2006**, *359*, 1673.
(11) Judd, D. A.; Nettles, J. H.; Nevins, N.; Snyder, J. P.; Liotta, D. C.; Tang, J.; Ermolieff, J.; Schinazi, R. F.; Hill, C. L. *J. Am. Chem. Soc.* **2001**, *123*, 886.
(12) Kim, G. S.; Judd, D. A.; Hill, C. L.; Schinazi, R. F. *J. Med. Chem.* **1994**, *37*, 816.
(13) Sarafianos, S. G.; Kortz, U.; Pope, M. T.; Modak, M. J. *Biochem. J.* **1996**, *319*, 619.

10.1021/ja804823g CCC: $40.75

tions of infectious prions in blood and cerebrospinal fluid.[14] Selective interaction of POMs with basic fibroblast growth factor, a globular single-chain heparin-binding polypeptide synthesized by different cell types, has also been demonstrated.[15]

The broad spectrum of biological activity combined with generally low cytotoxicity makes POMs attractive as potential therapeutic agents. However, considering the large number of biologically active POMs, there is very limited information on their mode of interaction on the molecular basis. It has been generally accepted that noncovalent binding influenced by the size, shape, and charge density of polyoxometalates is the main factor governing their biological activity, but on the other hand, very little is known about the reactivity of POMs toward biological molecules and their building blocks.

In our quest to gain more insight into the origins of the biological activity of this important class of compounds, we have focused our attention on the polyoxomolybdate $[Mo_7O_{24}]^{6-}$, also known as heptamolybdate. The well-established solution chemistry of polyoxomolybdates forms a good basis for studying interactions with biological model systems on a molecular level. Moreover, the first studies on the antitumor activity of POMs in general, revealed that the *in vivo* antitumoral activity of the polyoxomolybdate $[Mo_7O_{24}]^{6-}$, on several types of tumor cells is comparable to that of some commercial drugs.[16] The most recent studies have shown that $[Mo_7O_{24}]^{6-}$ exhibits potent antitumor activity against pancreatic cancer cells which are extremely resistant toward most of the known therapeutic agents.[18−20]

Several studies have revealed that molybdate binds to nucleotides exclusively via the phosphate group, leading to the formation of a pentamolybdodiphosphate type of structure.[21−25] At high temperatures the slight hydrolysis of mononucleotides in the presence of molybdate has been observed.[26] Polyoxomolybdates have also been shown to catalyze the hydrolysis of the labile "high energy" phosphoanhydride bonds in ATP.[27,28] Various studies implicate the interaction of molybdate with phosphate groups in ATP as one of the key factors in understanding the antitumor activity of $[Mo_7O_{24}]^{6-}$.[25,27,28] In our initial studies we examined the interactions between heptamolybdate and commonly used DNA model phosphodiesters.[29,30] The discovery of the phosphodiesterase activity of $[Mo_7O_{24}]^{6-}$ represents the first example of a phosphodiester bond cleavage promoted by a highly negatively charged polyoxometalate cluster. This encouraged us to further explore the reactivity of $[Mo_7O_{24}]^{6-}$ toward 2-hydroxypropyl-4-nitrophenyl phosphate (HPNP), which is commonly used as an RNA model system by means of ^{1}H, ^{31}P, and ^{95}Mo NMR, UV−vis, Raman, and Mo K-edge extended X-ray absorption fine structure (EXAFS) spectroscopy. EXAFS has been proven to be a very valuable technique in studying structures of polyoxometalates, since it can provide information about the coordination sphere of metal ions both in the solid state and in solution. A recent paper by Balula et al. gives a comprehensive overview of a number of studies which have been carried out in the past 10−15 years.[31]

Scheme 1. Chemical Structures of HPNP and $[Mo_7O_{24}]^{6-}$

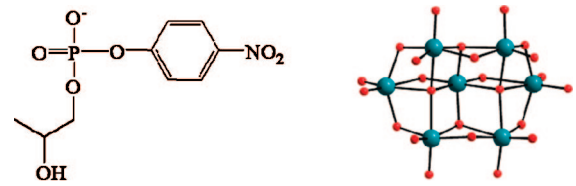

HPNP

$[Mo_7O_{24}]^{6-}$

In this study we demonstrate that contrary to the hydrolysis of bis(*p*-nitrophenyl)phosphate (BNPP), the transesterification of HPNP can be achieved under catalytic conditions, and we give a full account on the mechanism of this novel reaction (Scheme 1).

Experimental Section

Materials. Disodium *p*-nitrophenyl phosphate and 1,2-epoxypropane were obtained from Aldrich Ltd. Aqueous ammonia and barium hydroxide (Acros) were used to adjust pH in the synthesis of HPNP. The pH of the solutions for the NMR studies was adjusted with D_2SO_4 and NaOD, both from Acros. D_2O with 0.05 wt % 3-(trimethylsilyl) propionic acid (Acros) as an internal standard was used as a solvent. HPNP was prepared from *p*-nitrophenyl phosphate and 1,2-epoxypropane according to a published procedure.[32]

NMR Spectroscopy. ^{1}H, ^{31}P, and ^{13}C NMR spectra were recorded on a Bruker Avance 300 spectrometer and on a Bruker Avance 400 spectrometer. Trimethyl phosphate was used as a 0 ppm ^{31}P reference. ^{95}Mo NMR spectra were recorded on a Bruker Avance 600 (39 MHz) spectrometer.

Raman and UV−Visible Spectroscopy. FT-Raman spectra were recorded on a Bruker IFS-66 with a FRA106 Raman module (Nd:YAG laser). Typically 200 scans were taken with a resolution of 4 cm^{-1}. UV−vis absorption spectra have been measured on a Varian Cary 5000 spectrophotometer.

EXAFS Spectroscopy. EXAFS measurements were performed in transmission mode using a Si(111) double crystal monochromator on the Dutch-Belgian Beamline (DUBBLE, BM26A) at the European Synchrotron Radiation Facility (ESRF, Grenoble, France). Preliminary measurements were done during project 26 01 743 between March 6th and 10th, 2006. The ESRF storage ring was then operating under uniform filling mode. Energy resolution d*E*/*E*

(14) Lee, I. S.; Long, J. R.; Prusiner, S. B.; Safar, J. G. *J. Am. Chem. Soc.* **2005**, *127*, 13802.
(15) Wu, Q.; Wang, J.; Zhang, L.; Hong, A.; Ren, J. S. *Angew. Chem., Int. Ed.* **2005**, *44*, 4048.
(16) Fujita, H.; Fujita, T.; Sakurai, T.; Seto, Y. *Chemotherapy* **1992**, *40*, 173.
(17) Yamase, T.; Fujita, H.; Fukushima, K. *Inorg. Chim. Acta* **1988**, *151*, 15.
(18) Ogata, A.; Mitsui, S.; Yanagie, H.; Kasano, H.; Hisa, T.; Yamase, T.; Eriguchi, M. *Biomed. Pharmacother.* **2005**, *59*, 240.
(19) Yanagie, H.; Ogata, A.; Mitsui, S.; Hisa, T.; Yamase, T.; Eriguchi, M. *Biomed. Pharmacother.* **2006**, *60*, 349.
(20) Ogata, A.; Yanagie, H.; Ishikawa, E.; Morishita, Y,; Mitsui, S.; Yamashita, A.; Hasumi, K.; Takamoto, S.; Yamase, T.; Eriguchi, M. *Br. J. Cancer,* **2008**, *98*, 399.
(21) Katsoulis, D. E.; Lambriandou, A. N.; Pope, M. T. *Inorg. Chim. Acta* **1980**, *46*, L55.
(22) Geraldes, C. F. G. C.; Castro, M. C. C. A. *J. Inorg. Biochem.* **1986**, *28*, 319.
(23) Piperaki, P.; Katsaros, N.; Katakis, D. *Inorg. Chim. Acta* **1982**, *67*, 37.
(24) Hill, L. M. R.; George, G. N.; Duhm-Klair, A. K.; Young, C. G. *J. Inorg. Biochem.* **2002**, *88*, 274.
(25) Kwak, W.; Pope, M. T.; Scully, T. F. *J. Am. Chem. Soc.* **1975**, *97*, 5735.
(26) Cartuyvels, E.; Van Hecke, K.; Van Meervelt, L.; Görller-Walrand, C.; Parac-Vogt, T. N. *J. Inorg. Biochem.* **2008**, *102*, 1589.
(27) Weil-Malherbe, H.; Green, R. H. *Biochem. J.* **1951**, *49*, 3286.
(28) Ishikawa, E.; Yamase, T. *J. Inorg. Biochem.* **2006**, *100*, 344.
(29) Cartuyvels, E.; Absillis, G.; Parac-Vogt, T. N. *Chem. Commun.* **2008**, 85.
(30) Van Lokeren, L.; Cartuyvels, E.; Absillis, G.; Willem, R.; Parac-Vogt, T. N. *Chem. Commun.* **2008**, 2774.
(31) Balula, M. S. S.; Santos, I. C. M. S.; Gamelas, J. A. F.; Cavaleiro, A. M. V.; Binsted, N.; Schlindwein, W. *Eur. J. Inorg. Chem.* **2007**, 1027, and references therein.
(32) Brown, D. M.; Usher, D. A. *J. Chem. Soc.* **1965**, 6558.

is 2×10^{-4}. The final solutions were measured during in-house beam time on November 21st and 22nd, 2007 at the same beamline, under identical operating conditions. Higher harmonics were rejected by the Si mirrors (suppression factor about 1000). The molybdenum K-edge spectra were collected using Oxford Instruments ionization chambers filled with 30% Ar/70% He at 1 bar for I_0 and pure Ar at 1.5 bar for I_t at ambient temperature and pressure. Data were collected in equidistant k-steps of 0.05 $Å^{-1}$ across the EXAFS region. A Mo metal foil (first inflection point at 19999 eV) was used for energy calibration.

As the Mo phase function is strongly nonlinear at k values below $k = 5$ $Å^{-1}$, in a first approach, the filtering and back-transformation procedure was made by using only k values larger than $k = 5$ $Å^{-1}$ (k range was then 5−16.9 $Å^{-1}$), but this had only a minor effect on the structural parameters obtained. Therefore, it was decided to use the whole k range from 2.6 to 16.9 $Å^{-1}$ in the final procedure.

Solutions of the polyoxomolybdates were sealed in polyethylene cuvets with a path length of 8 mm. Calculations had indicated that $[Mo_7O_{24}]^{6-}$ concentrations of 25 mM (corresponding to a Mo concentration of 175 mM) would result in an edge jump between 0.9 and 1 for a path length of 8 mm. The concentration of the reaction solution was 100 mM in HPNP and 25 mM in $[Mo_7O_{24}]^{6-}$, and the samples were diluted before the measurement.

EXAFS data extraction and data fitting were performed using the program EXAFSPAK.[33] Theoretical phase and amplitude functions were calculated using FEFF 8.2 using the crystal structure from ref 58.[34] The amplitude reduction factor, S_0^2, was kept constant at 1 throughout the fit.

Kinetics. In a typical kinetic experiment, the hydrolysis of HPNP (50 mM, D_2O solution) in the presence of varying concentrations of molybdate was followed by ^{1}H NMR spectroscopy. The pH of the solution was measured in the beginning and at the end of the hydrolytic reaction and the difference was typically less than 0.1 pH unit. The pD value of the solution was obtained by adding 0.41 to the pH reading, according to formula pD = pH + 0.41.[35] The reaction samples were kept at constant temperature (typically 37 or 50 °C) and the rate constants for the hydrolysis were determined by following the appearance of the p-nitrophenol resonances in the ^{1}H NMR spectra at different time intervals. The observed first order rate constants (k_{obs}) were calculated by the integral method from at least 90% conversion. For reactions performed in H_2O solutions, the same kinetic method was used, and the reaction products were detected by ^{1}H NMR water suppression technique. The Michaelis−Menten kinetic measurements were performed on samples which contained a fixed concentration of $[Mo_7O_{24}]^{6-}$ (25 mM) while the concentration of HPNP was increased from 5 to 625 mM. The inhibition experiments were performed by adding increasing amounts of dimethyl phosphate (from 0 to 2.5 M) to a solution containing equimolar amounts (25 mM) of $[Mo_7O_{24}]^{6-}$ and HPNP in D_2O solution and determining the hydrolysis rate constants for each step as described above.

Results and Discussion

Cleavage of HPNP by $[Mo_7O_{24}]^{6-}$. $[Mo_7O_{24}]^{6-}$ is formed by the acidification of an aqueous molybdate solution to a pH below 6 (eq 1).[33,37] The solution chemistry of $[Mo_7O_{24}]^{6-}$ has been extensively studied and the thermodynamic parameters published elsewhere can be used for the estimation of the $[Mo_7O_{24}]^{6-}$ concentration under different reaction conditions[36−38] (see Supporting Information). Although the models for the speciation of molybdate solutions are well-established and based on reliable and reproducible data,[36,37] it has to be noted that the accurate experimental determination of the $[Mo_7O_{24}]^{6-}$ concentration is still rather difficult since different factors such as the starting concentration of molybdate, salt concentration, temperature, and pH of the solution will have an influence on the equilibrium shown in eq 1.

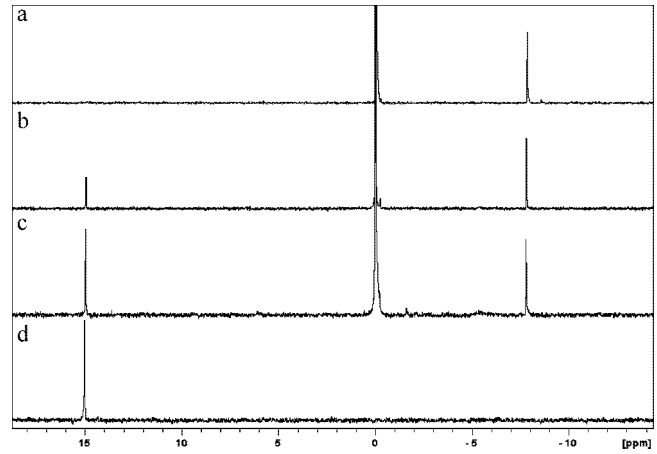

Figure 1. ^{31}P NMR spectra of a D_2O solution containing equimolar amounts of HPNP and $Na_6[Mo_7O_{24}]$ (50 mM, pD 5.7, $T = 50$ °C, using $(CH_3)_3PO$ as a 0 ppm reference) measured at (a) 1 h, (b) 27 h, (c) 2 days, and (d) 12 days after mixing. The k_{obs} for the HPNP hydrolysis calculated by integrating the ^{31}P NMR signal of the initial HPNP-$[Mo_7O_{24}]^{6-}$ complex afforded virtually the same value (6.47×10^{-6} s^{-1}) as k_{obs} calculated by measuring the peak area of p-nitrophenol peaks in ^{1}H NMR (6.53×10^{-6} s^{-1}). See text for the assignment of the ^{31}P NMR resonances.

$$7[MoO_4]^{2-} + 8H^+ \rightleftharpoons [Mo_7O_{24}]^{6-} + 4H_2O \qquad (1)$$

The model reactions between HPNP and $[Mo_7O_{24}]^{6-}$ have been performed under conditions which ensure a high concentration of $[Mo_7O_{24}]^{6-}$ in solution (pD = 5.9, 400 mM starting concentration of MoO_4^{2-}). Indeed, ^{95}Mo NMR of the solution revealed only a sharp line at 0.3 ppm corresponding to $[MoO_4]^{2-}$ and a broad resonance at 32 ppm which could be unambiguously assigned to the heptamolybdate structure.[39] Discriminating between $[Mo_7O_{24}]^{6-}$ and $[HMo_7O_{24}]^{5-}$ is not possible by means of ^{95}Mo NMR spectroscopy.[39]

Under these conditions, the cleavage of HPNP proceeded smoothly. During the course of the reaction ^{1}H NMR spectra of the aromatic region indicated the disappearance of HPNP resonances at 8.27 and 7.36 ppm and the appearance of p-nitrophenol (NP) resonances, which is clear evidence that the cleavage of the more labile phosphoester bond in HPNP occurred. The product of hydrolysis, p-nitrophenol, was easily detected by its characteristic NMR resonances at 8.19 and 6.98 ppm. Similarly, ^{31}P NMR spectroscopy indicated the disappearance of the HPNP resonance at −7.92 ppm and the appearance of a new peak at 15.1 ppm, which could be unambiguously assigned to the cyclic phosphate ester (CycP) (Figure 1).[40]

The formation of the cyclic phosphate ester was also evidenced in ^{1}H NMR spectra where the appearance of the

(33) George, N. G.; Pickering, I. J. *EXAFSPAK, a suite of computer programs for analysis of X-ray absorption spectra*; Stanford Synchrotron Radiation Laboratory: Stanford, CA, 2000.
(34) Ankudinov, A. L.; Ravel, B.; Rehr, J. J.; Conradson, S. D. *Phys. Rev. B* **1998**, *58*, 7565.
(35) Glasoe, P. K.; Long, F. A. *J. Phys. Chem.* **1960**, *64*, 188.
(36) Cruywagen, J. J. *Advan. Inorg. Chem* **2000**, *49*, 127, and references therein.
(37) Pope, M. T. *Heteropoly and Isopoly Oxometalates;* Springer: Berlin, 1983; pp 60−117.
(38) Cruywagen, J. J.; Draaijer, A. G.; Heyns, J. B. B.; Rohwer, E. A. *Inorg. Chim. Acta* **2002**, *331*, 322.
(39) Maksimovskaya, R. I.; Maksimov, G. M. *Inorg. Chem.* **2007**, *46*, 3688.
(40) Chandrasekhar, V.; Deria, P.; Krishnan, V.; Athimoolan, A.; Singh, S.; Madhavaiah, C.; Srivatsan, S. G.; Verma, S. *Bioorg. Med. Chem. Lett.* **2004**, *14*, 1559.

Scheme 2. Transesterification of HPNP Promoted by $[Mo_7O_{24}]^{6-}$

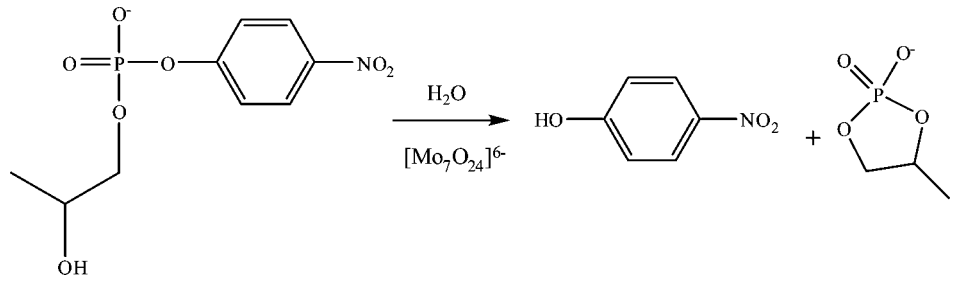

methyl peak of the cyclic product could be detected at 1.35 ppm during the course of the reaction. The results are consistent with the reaction scheme shown in Scheme 2, in which *p*-nitrophenol and the cyclic phosphate ester are the only two products of HPNP cleavage.

The rate constant for the cleavage of HPNP was calculated by integration of the NP resonances and its value, $k_{obs} = 6.62 \times 10^{-6}$ s^{-1} ($T = 50$ °C and pD 5.9) represents an acceleration of nearly 40 times compared to the uncatalyzed cleavage of HPNP under the same conditions ($k_{obs} = 1.78 \times 10^{-7}$ s^{-1}). It is important to note that the NMR spectra did not show evidence of any paramagnetic species, which excludes the possibility of oxidative cleavage and the reduction of Mo(VI) to Mo(V). Close examination of the Mo K-edge XANES spectra of three representative solutions (solution A, at the beginning of the reaction, solution B, in the middle of the reaction, and solution C, at the end of the reaction) showed identical traces in all three cases, indicating that no change in the oxidation state of the molybdenum atoms takes place during the reaction. When the reaction was followed by UV−vis spectroscopy, the only change observed during the course of the reaction was the appearance of yellow *p*-nitrophenol with its characteristic peak at 315 nm. The appearance of "blue species" was not observed during any point of reaction. This indicates that the hydroxyl group in HPNP did not cause oxidation and degradation of $[Mo_7O_{24}]^{6-}$, as it has been previously observed in reactions of heptamolybdate with some alcohols.[41]

pD Dependence of the Hydrolysis Rate. The effect of pD on the cleavage reaction was examined to correlate the rate-pH profile with the species distribution diagram. The fact that reactivity follows the pD profile of a certain species suggests that k_{obs} is proportional to the concentration of that given species. Since the kinetic measurements were performed in D_2O solutions, the rates were plotted as a function of pD, which was obtained by adding 0.41 pH units to the recorded pH value.[35] This is illustrated in Figure 2, where the values of k_{obs} and the fraction of polyoxometalate species are plotted as a function of pL (L = H,D).

As it can be seen in Figure 2, the pD dependence of k_{obs} exhibits a bell-shaped profile, with the fastest cleavage observed at pD 5.9. Comparison of the rate profile with the concentration profile of polyoxometalates shows a striking overlap of the k_{obs} profile with the concentration of heptamolybdate,[36−39] strongly suggesting that $[Mo_7O_{24}]^{6-}$ is the hydrolytically active species. Although at the examined pD range other molybdenum(VI) species such as $[MoO_4]^{2-}$ and $[Mo_8O_{26}]^{4-}$ are present in solution, they seem to be catalytically much less active. Slow hydrolysis at lower pD values, where $[Mo_8O_{26}]^{4-}$ predominates, implies low catalytic activity of this species. Since at pD 8.4, where $[MoO_4]^{2-}$ is the only Mo(VI) species present in solution, HPNP hydrolysis occurred at rates comparable to the background cleavage we could conclude that the monomeric $[MoO_4]^{2-}$ form is virtually hydrolytically inactive.

Binding of HPNP to $[Mo_7O_{24}]^{6-}$. Acceleration of HPNP hydrolysis in the presence of $[Mo_7O_{24}]^{6-}$ implies that interaction between HPNP and $[Mo_7O_{24}]^{6-}$ must take place in solution. At first glance this seems counterintuitive since highly negatively charged metal clusters are not expected to bind or interact with anions. The ^{31}P NMR spectrum of HPNP showed very little change upon addition of $[Mo_7O_{24}]^{6-}$ indicating fast exchange on the NMR time scale between free and bound HPNP. Therefore in the next step, kinetic experiments using a fixed amount of $[Mo_7O_{24}]^{6-}$ (25 mM) and increasing amounts of HPNP at pD 5.9 and 50 °C were performed. The results shown in Figure 3, reveal only slight signs of curvature at 625 mM HPNP. The data fit the general Michaelis−Menten reaction scheme (Scheme 3), where $[Mo_7O_{24}]^{6-}$ is a catalyst, permitting the calculation of kinetic K_m and V_{max} parameters. The values for $K_m = 1.06$ M and $k_2 = 3.02 \times 10^{-4}$ s^{-1} were obtained by a computer generated least-squares fit of k_{obs} to eq 2.

$$V = k_2[E]_0 \frac{[HPNP]}{[HPNP] + K_m} \qquad (2)$$

The binding between HPNP and $[Mo_7O_{24}]^{6-}$ appears to be much weaker than that between HPNP and highly positively charged complexes such as trinuclear complexes formed from a polypyridyl ligand L, $[(L-H)Co^{II}Cu_2]^{5+}$ and $[(L-H)Co^{III}(NO_2)_2Cu_2]^{4+}$ which have binding constants in the range between 470 and 820 M^{-1}.[42]

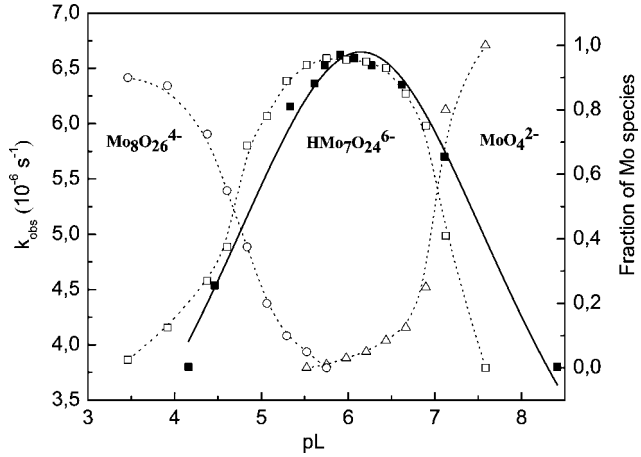

Figure 2. pD dependence of k_{obs} (■, solid line) for the cleavage of HPNP (50 mM) in the presence of Na_2MoO_4 (400 mM starting concentration) in D_2O. Fractions of molybdate species (□, ○, △, dotted line) determined for H_2O solutions as a function of pH are added for comparison.

(41) Yamase, T. *J. Chem. Soc., Dalton. Trans.* **1991**, *11*, 3055.
(42) Fritsky, I. O.; Ott, R.; Pritzkow, H.; Krämer, R. *Inorg. Chem. Acta* **2003**, *346*, 111.

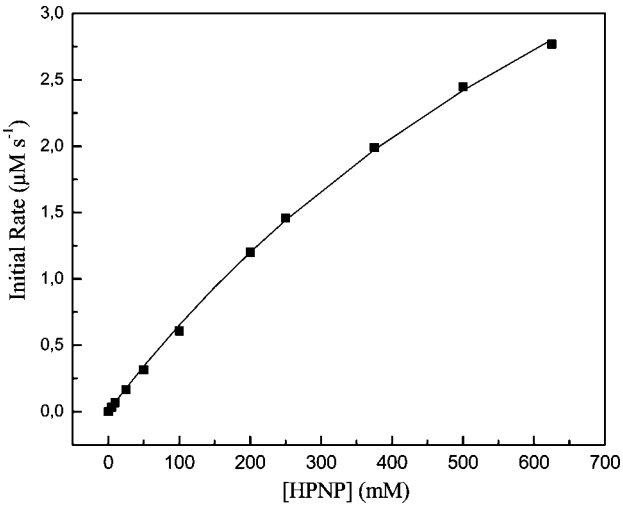

Figure 3. Saturation kinetics studies for the hydrolysis of HPNP in the presence of 25 mM $[Mo_7O_{24}]^{6-}$ at pD 5.9 and $T = 50$ °C.

Scheme 3. Kinetic Scheme for the Hydrolysis of HPNP

$$\text{HPNP} + [Mo_7O_{24}]^{6-} \underset{k_{-1}}{\overset{k_1}{\rightleftharpoons}} \text{HPNP---}[Mo_7O_{24}]^{6-} \overset{k_2}{\rightleftharpoons} \text{NP} + \text{CycP}$$

The nature of the HPNP−$[Mo_7O_{24}]^{6-}$ complex is difficult to assess. While the interactions between $[Mo_7O_{24}]^{6-}$ and various monophosphates or monophosphonates have been well understood, the interactions with the bis-substituted phosphates have been virtually unexplored and to the best of our knowledge no data in literature are available on this type of complexes. Binding of phosphate, monosubstituted phosphates, and phosphonates to $[Mo_7O_{24}]^{6-}$ leads to the formation of a pentamolybdodiphosphate structure $[(RP)_2Mo_5O_{23}]^{6-}$ that is composed of five MoO_6 octahedra coupled by one corner-shared and four edge-shared contacts to form a ring structure, which is capped on either side by two phosphate moieties.[43−48] The formation of a pentamolybdodiphosphate structure is best reflected in ^{31}P NMR spectra of monophosphonates that show large shifts (up to 7 ppm) in the ligand ^{31}P NMR resonances upon complexation.[44]

^{31}P NMR spectra of the reaction mixture recorded at variable temperatures were further used to study the interaction between HPNP and the heptamolybdate. Addition of $Na_6[Mo_7O_{24}]$ to HPNP at room temperature causes the ^{31}P NMR signal to shift by only 0.1 ppm, which is inconsistent with the formation of the pentamolybdodiphosphate structure.[44] However, variable temperature ^{31}P NMR spectra of a reaction mixture recorded immediately upon mixing, revealed consistent broadening of the HPNP ^{31}P resonance upon increase of temperature, suggesting the dynamic exchange process between free and bound HPNP at higher temperatures (Figure 4).

An alternative way to test the ability of the catalyst to bind to the substrate is to measure the inhibitory effect of a nonreactive substrate analogue.[49,50] To examine the influence of an inhibitor on the rate of hydrolysis, the normalized (k_{obs}/k_0) rate constants for the hydrolysis of HPNP were plotted as a function of increasing amounts of dimethyl phosphate (DMP) (Figure 5). The binding of DMP to $[Mo_7O_{24}]^{6-}$ appears to be so weak that even at 100 molar excess of the inhibitor, the rate constant for the hydrolysis of HPNP was only decreased by 45% compared to its value in the absence of DMP. Therefore it is reasonable to assume that the formation of a complex between $[Mo_7O_{24}]^{6-}$ and DMP does not significantly change the concentration of free DMP. This makes it possible to work with inhibitor concentrations that are much higher than the concentration of the catalyst and to fit the data represented in Figure 5 to eq 3 derived for competitive inhibition.

$$\frac{k_{obs}}{k_0} = \frac{K_I}{K_I + [\text{DMP}]} \tag{3}$$

The value obtained for K_I ($K_I = 3.29$ M) is in the same order of magnitude as the value obtained for HPNP binding to the

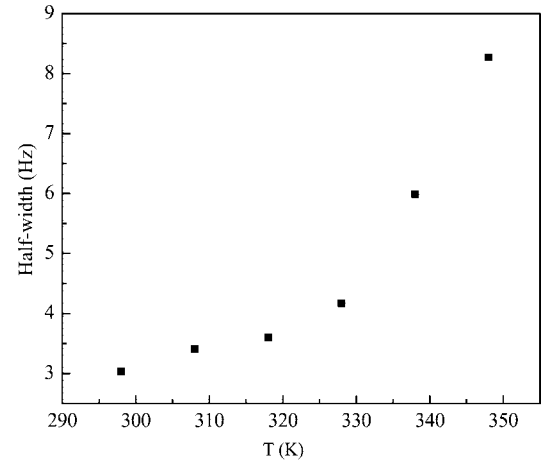

Figure 4. Half-width ($\nu_{1/2}$) of the ^{31}P NMR resonance of HPNP (25 mM, pD 5.6) in the presence of an equimolar amount of $Na_6[Mo_7O_{24}]$ plotted as a function of temperature.

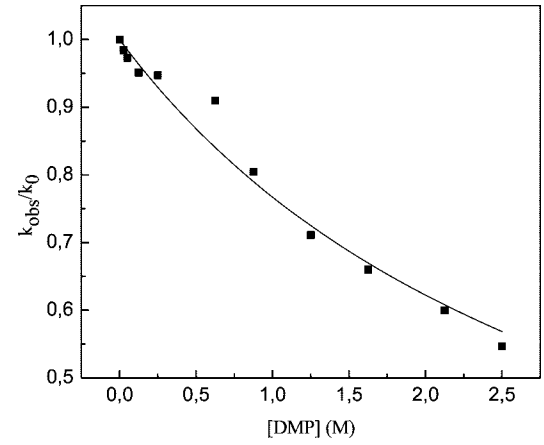

Figure 5. Ratio of the rate constant for the hydrolysis of HPNP catalyzed by 25 mM $[Mo_7O_{24}]^{6-}$ in the presence of dimethyl phosphate, DMP (k_{obs}), to the rate constant measured in the absence of DMP (k_0) at pD 5.9, 50 °C, and 25 mM HPNP.

(43) Lyxell, D. G.; Pettersson, L.; Persson, I. *Inorg. Chem.* **2001**, *40*, 584.
(44) Yagasaki, A.; Andersson, I.; Pettersson, L. *Inorg. Chem.* **1987**, *26*, 3926.
(45) Hill, L. M. R.; George, G. N.; Duhm-Klair, A. K.; Young, C. G. *J. Inorg. Biochem.* **2002**, *88*, 274.
(46) Kwak, W.; Pope, M. T.; Scully, T. F. *J. Am. Chem. Soc.* **1975**, *97*, 5735.
(47) Pettersson, L.; Andersson, I.; Öhman, L.-O. *Inorg. Chem.* **1986**, *25*, 4726.
(48) Strandberg, R. *Acta Chem. Scand.* **1973**, *27*, 1004.
(49) Iranzo, O.; Kovalevsky, A. Y.; Morrow, J. R.; Richard, J. P. *J. Am. Chem. Soc.* **2003**, *125*, 1988.
(50) Aquillar-Perez, F.; Gomez-Tagle, P.; Collado-Fregoso, E.; Yatsimirsky, A. Y. *Inorg. Chem.* **2006**, *45*, 9502.

complex. The slightly higher affinity for the binding of HPNP may be due to secondary interactions between hydroxyl group of HPNP and the $[Mo_7O_{24}]^{6-}$, which in the case of DMP are not possible.

In addition, a strong negative salt effect on the rate of HPNP hydrolysis was observed in the presence of two different salts (see Supporting Information). This can be related to the Olson−Simonson effect occurring for reactions between ions of the same sign, which predicts a rate decrease upon increasing the concentration of oppositely charged ions.[51]

Temperature Dependence of the Hydrolytic Reaction. The effect of temperature on the hydrolytic reaction was determined by measuring the temperature dependence of k_{obs}. As expected, at higher temperatures increased rates have been observed. Activation Gibbs function ($\Delta G^{\ddagger} = 183.4$ kJ mol^{-1} at 37 °C), enthalpy ($\Delta H^{\ddagger} = 85.47$ kJ mol^{-1}) and entropy ($\Delta S^{\ddagger} = -315.92$ J mol^{-1} K^{-1}) were obtained from the Arrhenius plot. While there is a close correspondence in the $\Delta H^{\ddagger}$ value to the values previously reported for the hydrolysis of BNPP, catalyzed by various metal complexes, the negative $\Delta S^{\ddagger}$ value is 2 to 3 times higher.[52−56] The negative value of activation entropy typically implies a largely ordered transition state and the increase of coordination number of phosphorus from four to five through formation of a trigonal−bipyramidal transition state. The much larger negative $\Delta S^{\ddagger}$ values observed in the hydrolysis of HPNP can be explained by the increased associative character of the transition state compared to the BNPP hydrolysis. This may arise from the fact that in the case of HPNP the attacking OH^- nucleophile comes from the HPNP ligand, while in the case of BNPP the OH^- nucleophile is coordinated to the metal complex and depending on the steric bulk of the ligand, may not be easily accessible. However, the activation parameters need to be interpreted with caution, as they are usually derived from the composite rate constants that also include contribution from the binding of the ligand to the complex. Activation entropy is considered to be a mixture of factors (changes in solvation, conformation, molecularity, ...) that cannot be rationalized or predicted.[52−56] Therefore it is difficult to assess whether the changes in activation entropy reflect changes in reaction mechanism or are due to changes in the binding of the phosphodiester to the metal complex.

Catalytic Turnover. Comparison of Raman spectra recorded in the beginning and after completion of hydrolysis were nearly identical, suggesting that the hydrolysis of HPNP did not result in a large modification of the heptamolybdate structure (Figure 6).[57]

This is in sharp contrast to the $[Mo_7O_{24}]^{6-}$-promoted hydrolysis of BNPP, in which inorganic phosphate as a product of hydrolysis, further reacts with heptamolybdate to give the hydrolytically inactive $[P_2Mo_5O_{23}]^{6-}$ complex.[29] Because of this undesired reaction, a catalytic turnover for the hydrolysis of (*p*-nitrophenyl)phosphate (NPP) and BNPP could not be achieved.

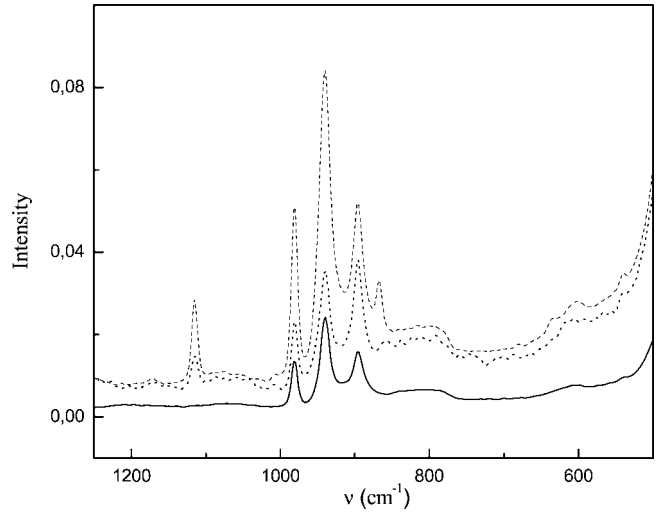

Figure 6. Raman spectra of a mixture containing equimolar amounts of HPNP and $[Mo_7O_{24}]^{6-}$ (25 mM, pH 5.3, $T = 50$ °C), recorded immediately upon mixing (dotted line) and at the end of hydrolytic reaction (dashed line). Raman spectrum of $[Mo_7O_{24}]^{6-}$ is added for comparison (solid line).

Table 1. Dependence of k_{obs} for the Hydrolysis of 50 mM HPNP on the Concentration Ratio HPNP/$[Mo_7O_{24}]^{6-}$ at $T = 50$ °C, pD 5.7

HPNP/$[Mo_7O_{24}]^{6-}$	$10^6 \times k_{obs}$ (s^{-1})
1:0.1	3.91
1:0.2	4.22
1:0.5	5.11
1:0.8	5.85
1:1.0	6.39

Since the transesterification of HPNP does not result in the formation of inorganic phosphate, $[Mo_7O_{24}]^{6-}$ should remain unaffected during the hydrolytic reaction, suggesting the possibility for a catalytic turnover. Indeed, full hydrolysis of 10 equiv of HPNP was achieved in the presence of only 1 equiv of $[Mo_7O_{24}]^{6-}$ (Table 1). Although modest, this turnover number of 10 proves that the reaction is catalytic.

EXAFS Spectroscopy. The molybdenum K-edge (located at 19999 eV) was used to investigate the coordination sphere of the molybdenum atoms in the $[Mo_7O_{24}]^{6-}$ cluster during the catalytic cleavage of HPNP. Because of the relatively weak backscattering power of the phosphorus atom, it is virtually impossible to monitor the binding of HPNP to the $[Mo_7O_{24}]^{6-}$ cluster by Mo K-edge EXAFS spectroscopy. However, EXAFS can provide clear insight into the nature of the polyoxomolybdate present in solution. So, the question that we tried to address by EXAFS is whether or not the $[Mo_7O_{24}]^{6-}$ cluster stays intact during the catalytic reaction or if it is partially converted into other polyoxomolybdate forms. The presence of inorganic phosphate in solution, which is also a possible product of the HPNP hydrolysis, can lead to a conversion of $[Mo_7O_{24}]^{6-}$ into the $[P_2Mo_5O_{23}]^{6-}$ cluster. This possible loss of $[Mo_7O_{24}]^{6-}$ catalyst during the hydrolytic reaction has been monitored and investigated by Mo K-edge EXAFS spectroscopy.

The raw k^3 weighted Mo K-edge EXAFS spectrum and the corresponding Fourier transform of the starting solution (solution A) are shown in Figure 7. Peaks in the Fourier transform were not corrected for the phase shift.

The Fourier transform shows two distinctive sets of peaks: a first one, centered at about $R + \Delta = 1.3$ Å, corresponding to the overlapping Mo···O shells in the range of real distances

(51) Olson, A. R.; Simonson, T. R. *J. Chem. Phys.* **1946**, *17*, 1167.
(52) Deal, K. A.; Hengge, A. C.; Burstyn, J. N. *J. Am. Chem. Soc.* **1996**, *118*, 1713.
(53) Deck, K. M.; Tseng, T. A.; Burstyn, J. N. *Inorg. Chem.* **2002**, *41*, 669.
(54) Chin, J.; Banzszczyk, M.; Jubian, V.; Zou, X. *J. Am. Chem. Soc.* **1989**, *111*, 186.
(55) Jones, D. R.; Lindoy, L. F.; Sargeson, A. M. *J. Am. Chem. Soc.* **1983**, *105*, 7327.
(56) Fry, F H.; Fishermann, J.; Belousoff, M. J.; Spiccia, L.; Brügger, J. *Inorg. Chem.* **2005**, *44*, 941.
(57) Lyhamm, L.; Pettersson, L. *Chem. Scr.* **1977**, *12*, 142.

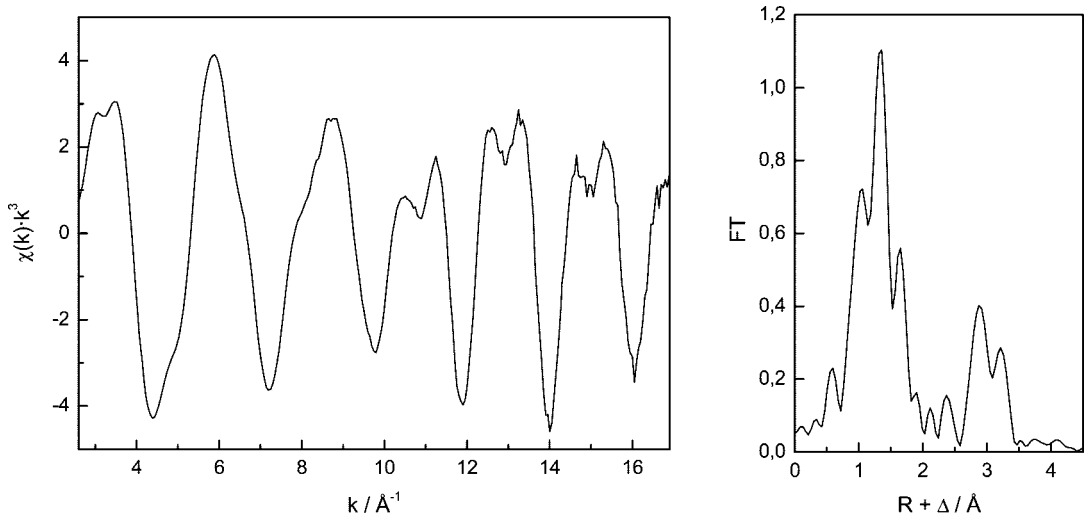

Figure 7. Raw k^3 weighted EXAFS (left) and corresponding Fourier transform (right) of the starting solution A.

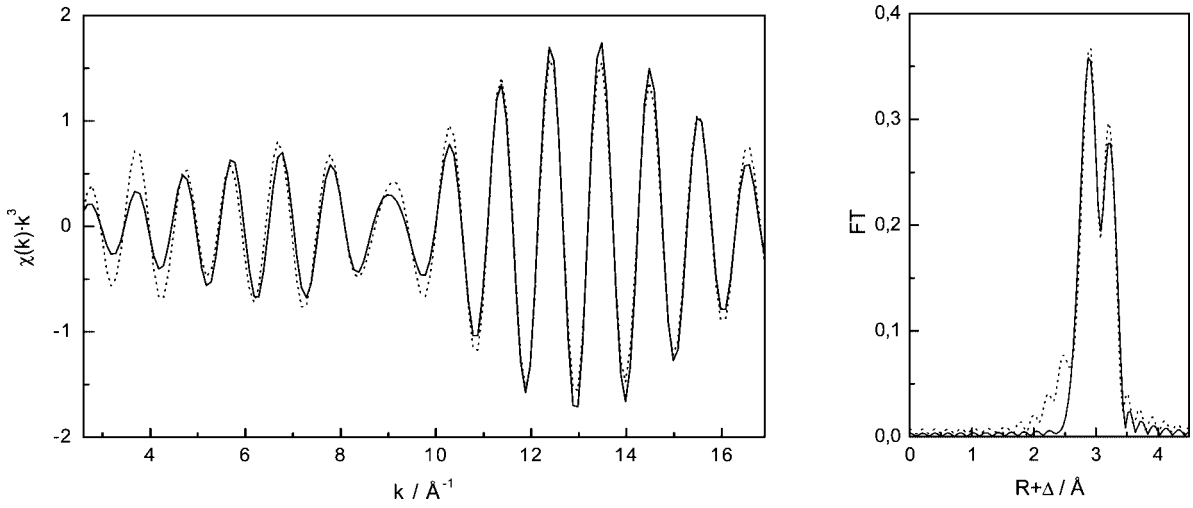

Figure 8. Back Fourier-transformed EXAFS signal (left) and Fourier transform window (right) taken from Figure 7. Solid line gives experimental curves; dotted line shows fitted curves.

1.7−2.4 Å and a second, centered at about R + Δ = 3 Å, which is split in two peaks, corresponding to the Mo···Mo shells at real distances of 3.2 and 3.4 Å, respectively.

Because the $[Mo_7O_{24}]^{6-}$ species is in constant equilibrium with the $[MoO_4]^{2-}$ monomer, it is not possible to obtain a reasonable fit including the Mo···O shells. The peaks at R + Δ = 3 Å, however, allow the identification of the polyoxomolybdate in solution. Indeed, close examination of the crystal structure of the $[Mo_7O_{24}]^{6-}$ cluster reveals that there are basically two sets of Mo···Mo distances in this molecule: one centered at 3.2 Å and another one centered at 3.4 Å.[58] In the $[P_2Mo_5O_{23}]^{6-}$ cluster, however, all Mo···Mo distances are more or less the same and centered at 3.4 Å.[49] So, monitoring the amplitude of the Mo···Mo shell at 3.2 Å allows us to follow the change in the concentration of $[Mo_7O_{24}]^{6-}$.

Therefore, a back-transformation from FT to $\chi(k)$ in the range of the Mo···Mo shells was made to give the corresponding EXAFS oscillations. These were then fitted with two Mo···Mo shells. This Fourier-filtered data range, taken from the spectra in Figure 7, is shown in Figure 8. The experimental curves are given as solid lines and the fitted curves are given as dotted lines. Careful calculation from the crystal data indicates that every Mo atom in the $[Mo_7O_{24}]^{6-}$ cluster "sees" on average 1.71 Mo neighbors at 3.2 Å and also 1.71 Mo neighbors at 3.4 Å. These coordination numbers N have been fixed in the shell fit procedure, whereas the distances R and Debye−Waller factors σ^2 were left free. The fitted distances of 3.23 and 3.40 Å, respectively, correspond well to the distances obtained from the crystal structure.

The EXAFS structural parameters were also determined for the reaction mixtures in which 50% of HPNP was hydrolyzed (solution B), and for the solution in which HPNP was fully hydrolyzed (solution C), and these results are summarized in Table 2.

To see whether there is a change in concentration of the $[Mo_7O_{24}]^{6-}$ cluster in the course of the reaction, the Debye−Waller factors obtained from the shell-fit procedure for solution A were taken and fixed for solution B, whereas the coordination numbers and distances were now left free. As can be seen from Table 2, the distances remain unaltered to less than 0.01 Å in a free fit, when compared to the starting solution. This indicates that no significant structural changes in the Mo···Mo shells occur between solutions A and B.

(58) Sjöbom, K.; Hedman, B. *Acta Chem. Scand.* **1973**, *27*, 3673.

Table 2. EXAFS Structural Parameters for $[Mo_7O_{24}]^{6-}$−HPNP Solutions at Different Stages of Hydrolytic Reaction

	N^a	R^a (Å)	σ^2 (Å^2)	ΔE (eV)	F^c
solution A	1.71[b]	3.23	0.00549	9.7	0.300
	1.71[b]	3.40	0.00600		
solution B	1.52	3.23	0.00549[b]	9.6	0.252
	1.59	3.40	0.00600[b]		
solution C	1.26	3.23	0.00549[b]	10.6	0.178
	1.52	3.40	0.00600[b]		

[a] Errors in coordination numbers N are ±10%; errors in distances R are ±0.01 Å. [b] Value fixed during shell-fit procedure. [c] Weighted F-factor (goodness of fit).

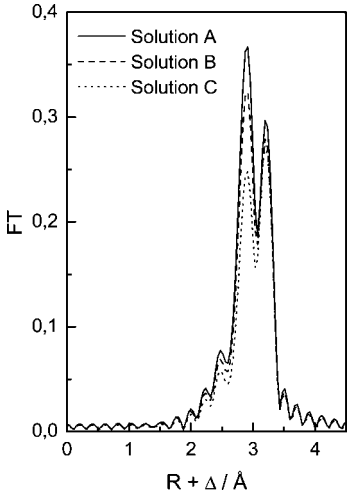

Figure 9. Combined fitted Fourier transform signals from solutions A, B, and C.

The k^3 weighted EXAFS and the corresponding Fourier transform window of solution B (see Supporting Information) indicated that the changes in amplitude compared to solution A are minimal, as can also be seen from Table 2, implying that only a small amount of the $[Mo_7O_{24}]^{6-}$ cluster has been decomposed at this point of the catalytic reaction.

The k^3 weighted EXAFS and the corresponding Fourier transform window of solution C which was taken at the end of the hydrolytic reaction (see Supporting Information) indicated a small decrease in the amplitude of the peak at 3.2 Å, as can also be seen in Table 2.

For the ease of comparison, Figure 9 shows a combined view of the fitted Fourier transform signals from solutions A, B, and C. As can be seen, the Mo···Mo shell at 3.4 Å is hardly changing (if one assumes that conversion of the $[Mo_7O_{24}]^{6-}$ cluster leads to the formation of small amounts of $[P_2Mo_5O_{23}]^{6-}$, no drastic changes in the Mo···Mo shell at 3.4 Å are expected). However, a small but gradual decrease of the Mo···Mo shell at 3.2 Å is seen, implying that about 25 ± 5% of the initial cluster is converted into $[P_2Mo_5O_{23}]^{6-}$, after the catalytic cleavage of HPNP has been completed. The phosphate ion, which is necessary for the formation of $[P_2Mo_5O_{23}]^{6-}$, is most likely a result of the partial hydrolysis of the second phosphoester bond in HPNP.

An alternative way of determining the speciation in solution could have consisted of putting together a library of EXAFS-spectra, including the limiting species $[MoO_4]^{2-}$, $[Mo_8O_{26}]^{4-}$, $[Mo_7O_{24}]^{6-}$, the P-containing cluster $[P_2Mo_5O_{23}]^{6-}$ and other possible P-containing species (if necessary). By using deconvolution techniques such as principal component analysis (PCA), the speciation of the intermediate solutions could then be expressed in terms of percentages of these species. However, we did not include the $[Mo_8O_{26}]^{4-}$ species in our sample series for the EXAFS measurements, because we could prove by ^{95}Mo NMR that this species is not present at the pH values of our sample series (pH 5.5). The ^{95}Mo NMR of the reaction mixture is given in the Supporting Information (Figure 7S). As can be seen from Figure 7S, there is no evidence for the existence of any $[Mo_8O_{26}]^{4-}$ cluster, which has a characteristic ^{95}Mo NMR shift at 90 ppm.[39] This is also fully in agreement with a number of potentiometric studies which all indicate that the $[Mo_8O_{26}]^{4-}$ species only starts to form around pH 4 and is the most dominant polyoxomolybdate anion at pH values below 3.[36,37] Furthermore, ^{31}P NMR measurements on solution C (corresponding to the end of the reaction) revealed that the $[P_2Mo_5O_{23}]^{6-}$ cluster, characterized by its ^{31}P NMR shift at −2.1 ppm (referenced to 85% H_3PO_4 as external standard) is the only molybdophosphate species present in that solution. This is fully in accordance with previous studies which have shown that under mildly acidic conditions the presence of free phosphate leads to the conversion of the heptamolybdate structure into the pentamolybdodiphosphate ion $[P_2Mo_5O_{23}]^{6-}$.[47] Therefore, as we were able to get detailed insight in the speciation in solution via NMR, we chose the alternative way of determining N via direct EXAFS measurements.

Proposed Mechanism. The mechanism of the metal-catalyzed hydrolysis of RNA model phosphate diesters has been investigated in great detail.[59−61] The generally accepted mechanism involves the participation of a metal-coordinated hydroxide as a general base catalyst. The kinetically equivalent mechanism would involve nucleophilic attack of the deprotonated hydroxy group of the substrate. There is emerging evidence that to a number of metal-catalyzed hydrolytic cleavages of HPNP the second mechanism applies.[59] A classical way to distinguish between a general base and the nucleophilic path is to determine the solvent deuterium isotopic effect (^Dk).[62−64] However, a detailed analysis of the ^Dk would require the exact determination of polyoxomolybdate speciation in the broad pL (L = H, D) range, which was proven to be a rather complex matter (see Supporting Information).

Considering the structure of $[Mo_7O_{24}]^{6-}$, chemical logic suggests that the catalyst cannot function by direct coordination of the alcoholic group to the metal ion that is followed by the subsequent nucleophilic attack of the deprotonated hydroxyl group. Until now, no examples of molybdenum(VI) coordinated to an alcoholic group in $[Mo_7O_{24}]^{6-}$ have been reported in the literature. On the other hand, the general base mechanism in metal-catalyzed hydrolysis of phosphate diesters presumes the presence of at least one metal-coordinated water molecule. Although in H_2O and D_2O solutions, $[Mo_7O_{24}]^{6-}$ undergoes protonation to give $[LMo_7O_{24}]^{5-}$ and $[L_2Mo_7O_{24}]^{6-}$ species (L = H, D), ^{17}O NMR studies suggest that the two possible protonation sites on $[Mo_7O_{24}]^{6-}$ involve triple- and double-

(59) Bonfa, L.; Gatos, M.; Manzin, F.; Tecilla, P.; Tonellato, U. *Inorg. Chem.* **2003**, *42*, 3943.
(60) Fritsky, I. O.; Ott, R.; Pritzkow, H. Kŕ.; amer, R. *Chem.—Eur. J.* **2001**, *7*, 1221.
(61) Molenveld, P.; Engbersen, J. F. G.; Kooijman, H.; Spek, A. L.; Reinhoudt, D. N. *J. Am. Chem. Soc.* **1998**, *120*, 6726.
(62) Gold, V., Ed. *Advances in Physical Organic Chemistry*; Academic Press: New York, 1967.
(63) Jones, D. R.; Lindoy, L. F.; Sargeson, A. M. *J. Am. Chem. Soc.* **1983**, *105*, 7327.
(64) Deal, K. A.; Burstyn, J. N. *Inorg. Chem.* **1996**, *35*, 2792.
(65) Yang, M. Y.; Iranzo, O.; Richard, J. P.; Morrow, J. R. *J. Am. Chem. Soc.* **2005**, *127*, 1064.

bridging oxygen atoms.[39] Therefore, since up to now, no evidence of water coordinated to molybdenum(VI) in $[Mo_7O_{24}]^{6-}$ exists, the question is then by which mechanism does $[Mo_7O_{24}]^{6-}$ promote the cleavage of HPNP? To gain more insight into the origin of the catalytic activity of $[Mo_7O_{24}]^{6-}$, we performed hydrolytic experiments with the analogous and isostructural $[W_7O_{24}]^{6-}$ polyoxometalate cluster. Our previous work has shown that despite the striking structural analogy between these two polyoxometalates, the $[W_7O_{24}]^{6-}$ cluster was found to be virtually inactive toward the hydrolysis of BNPP. Consequently, it was not surprising to observe that HPNP hydrolysis proceeded with rates comparable to the background cleavage, indicating that $[W_7O_{24}]^{6-}$ is also inactive toward HPNP hydrolysis. This further confirms our previous hypothesis that the origin of hydrolytic activity of $[Mo_7O_{24}]^{6-}$ may lie in its high internal lability. An intramolecular exchange process which results in partial detachment of one MoO_4 tetrahedron[39,66,67] may allow for the attachment of the structurally related phosphodiester tetrahedron into the polyoxometalate structure. This is analogous to the well-known process that occurs at higher temperatures in which tetrahedral molybdate adds to heptamolybdate to yield the octamolybdate structure.[66] Broadening of the ^{31}P NMR resonances of HPNP in the presence of $[Mo_7O_{24}]^{6-}$ upon increase of temperature is in agreement with the interaction between HPNP and $[Mo_7O_{24}]^{6-}$ taking place at elevated temperatures. The incorporation of the phosphodiester group of HPNP into the polyoxomolybdate skeleton results in the sharing of its oxygen atoms with Mo(VI) centers that can cause polarization and strain of the P−O ester bond, that in turn makes it more susceptible toward hydrolysis. This implies that water from the solvent acts as a nucleophile, and that the catalyst acts through destabilization of the phosphodiester bond through its incorporation into the polyoxometalate skeleton.

Conclusion

In conclusion, we report the first example of an RNA model phosphodiester bond cleavage promoted by a highly negatively charged polyoxometalate cluster. The hydrolysis of HPNP results in the formation of a cyclic product that has been identified by means of ^{1}H and ^{31}P NMR spectroscopy. The kinetic studies strongly suggest that $[Mo_7O_{24}]^{6-}$ is the hydrolytically active complex and that the cleavage occurs by a mechanism which is different to that of other currently known hydrolytically active metal complexes. The cleavage is catalytic, although the EXAFS data suggest that under catalytic conditions a partial conversion of $[Mo_7O_{24}]^{6-}$ into $[P_2Mo_5O_{23}]^{6-}$ takes place. The origin of the hydrolytic activity of heptamolybdate probably lies in its dynamic nature, which may allow for the interaction and incorporation of phosphodiester moieties into its skeleton. We are currently examining phosphoesterase activity of other types of polyoxometalate complexes. These studies focusing on the reactivity of polyoxometalates are important since they may shed more light on the molecular origin of their biological activity.

Acknowledgment. T.N.P.V. thanks FWO-Flanders (Belgium) for a fellowship. G.A. thanks FWO-Flanders (Belgium) for the doctoral fellowship. R.V.D. thanks the FWO-Flanders for a travel grant which allowed him to spend 6 months at the European Synchrotron Radiation Facility (ESRF, Grenoble, France). The authors thank the FWO-Flanders and the NWO for providing beam time at the DUBBLE facility (ESRF, Grenoble, France) and Dr. Wim Bras for providing an additional 6 shifts of in-house time. Sergey Nikitenko (DUBBLE) is acknowledged for technical support. C. Hennig (The Rossendorf Beamline, ESRF, Grenoble, France) is acknowledged for stimulating discussions about the EXAFS data treatment. Financial support has been provided by the K.U.Leuven (GOA 03/03).

Supporting Information Available: Model for the estimation of the $[Mo_7O_{24}]^{6-}$ concentration under different reaction conditions, influence of salt concentration on the hydrolysis rate, k^3 weighted EXAFS signals and Fourier transform of solution B and C, Mo K-edge XANES spectra for solutions A, B, and C, ^{95}Mo NMR spectrum of the reaction mixture, pH dependence of k_{obs}, and ^{17}O NMR spectra. This material is available free of charge via the Internet at http://pubs.acs.org.

JA804823G

(66) Howarth, O. W.; Kelly, P. *J. Chem. Soc., Chem. Commun.* **1988**, 1236.
(67) Howarth, O. W.; Kelly, P.; Pettersson, L. *J. Chem. Soc., Dalton Trans.* **1990**, 81.